Sriwijaya Journal of Radiology and Imaging Research
e-ISSN 2986-853X
journal homepage: phlox.or.id/index.php/sjrir

Original Research Article

Diffusion Tensor Imaging and Resting-State Functional MRI Reveal Coupled Microstructural and Default-Mode Network Alterations in Mild Cognitive Impairment: A Diagnostic Accuracy Study

Taryudi Suharyana[1*], Akmal Hasan[2], Jason Willmare[3]

[1]*Department of Neurology, CMHC Research Center, Palembang, Indonesia*
[2]*Department of Neurology, Phlox Institute, Palembang, Indonesia*
[3]*Department of Neurology, Diffa State Hospital, Diffa, Niger*

ARTICLE INFO

Article history:
Received: July 30, 2025
Accepted: September 15, 2025
Published: October 30, 2025

Reporting guideline:
STARD 2015 (diagnostic accuracy)

Keywords:
Cognitive dysfunction
Default mode network
Diffusion tensor imaging
Magnetic resonance imaging
White matter

***Corresponding author:**
Taryudi Suharyana
E-mail: taryudi.suharyana@cattleyacenter.id
ORCID: 0009-0000-2367-0670

DOI: 10.59345/sjrir.v3i2.285

ABSTRACT

Introduction: Early-stage neurodegeneration — clinically expressed as mild cognitive impairment (MCI) — lacks accessible imaging biomarkers that link microstructural white-matter injury to functional network disruption. We evaluated whether integrating diffusion tensor imaging (DTI) and resting-state functional MRI (rs-fMRI) at 3.0-Tesla improves detection of MCI and substantiates a structural-to-functional disconnection mechanism.

Methods: In this STARD-2015-compliant, prospective cross-sectional diagnostic accuracy study at a tertiary hospital in Palembang, Indonesia, 85 participants (45 MCI, 40 age-, sex- and education-matched controls) underwent single-scanner 3.0-T MRI. DTI metrics (fractional anisotropy [FA], mean diffusivity [MD]) were derived by tract-based spatial statistics and posterior-cingulate-seeded Default Mode Network (DMN) connectivity by CONN. Consensus clinical diagnosis (Petersen criteria) was the blinded reference standard. Diagnostic accuracy used ROC/DeLong AUC, Wilson 95% confidence intervals (CIs), Cohen κ, and multivariable logistic regression.

Results: Posterior-cingulum FA was lower (0.399 ± 0.058 vs 0.489 ± 0.052, p<0.001) and MD higher in MCI; PCC–mPFC connectivity was reduced (0.392 ± 0.124 vs 0.586 ± 0.136, p<0.001). FA discriminated MCI with AUC 0.903 (95% CI 0.831–0.974; sensitivity 82.2%, specificity 90.0%); a combined FA+FC model reached AUC 0.901 with sensitivity 95.6% and NPV 93.8% but did not exceed FA alone (DeLong p=0.90). FA and connectivity were strongly correlated (r=0.79, 95% CI 0.69–0.86, p<0.001). Inter-reader agreement was substantial (κ=0.74 and 0.67).

Conclusion: Multimodal 3.0-T DTI and rs-fMRI provides an accurate, radiation-free signature of early-stage neurodegeneration; the coupling between cingulum microstructure and DMN connectivity is consistent with structural disconnection being associated with functional decoupling and offers a deployable tool for tertiary referral centres.

All authors have reviewed and approved the final version of the manuscript.

1. Introduction

Mild cognitive impairment (MCI) represents the symptomatic predromal stage of neurodegenerative disease, a transitional window in which cognitive complaints exceed expectations for age yet functional independence is preserved. Accurate identification of this stage is clinically critical because it defines the population in which disease-modifying intervention is most likely to succeed. A recent meta-analysis estimated the worldwide prevalence of MCI among community dwellers aged 50 years and older at roughly 15–20%,[1] and because emerging lifestyle and pharmacological interventions appear most effective when started early, the predromal window has become a focus of biomarker research.[2]

Conventional structural MRI is comparatively insensitive to the earliest changes of neurodegeneration, which are microstructural and connectional rather than volumetric. Diffusion tensor imaging (DTI) characterises white-matter integrity: fractional anisotropy (FA) declines and mean diffusivity (MD) rises as myelin and axonal architecture degrade, with the posterior cingulum and fornix affected early.[3-5] Resting-state functional MRI (rs-fMRI) maps spontaneous low-frequency co-fluctuation of the blood-oxygen-level-dependent signal and is especially powerful for interrogating the Default Mode Network (DMN), whose posterior cingulate cortex (PCC) and medial prefrontal cortex (mPFC) hubs lose synchrony early in disease.[6,7]

Prior diagnostic studies report DTI areas under the curve commonly between 0.80 and 0.90 for the best-performing tracts and consistently reduced posterior-DMN connectivity on rs-fMRI.[5,8] Multimodal fusion of structural and functional features can improve characterisation and prediction of conversion, although incremental

discrimination over the single best biomarker is often modest because the measures are correlated.[9] Critically, the direct correlation between tract microstructure and network connectivity — the structural–functional coupling that would substantiate a disconnection mechanism — is seldom tested within the same participants.[10-12] Accessible imaging biomarkers that track this early tissue change are therefore needed to complement molecular markers.[13]

These questions carry particular weight in Southeast Asia, where access to advanced neuroimaging remains uneven and concentrated in tertiary referral centres, and prospective multimodal data from Indonesian populations scanned on standard clinical 3.0-T systems are scarce.[8] We therefore conducted a prospective, STARD-2015–compliant diagnostic accuracy study integrating DTI and rs-fMRI in a single matched cohort at a tertiary hospital in Palembang, Indonesia, to quantify the diagnostic accuracy of individual and combined biomarkers for MCI against a blinded clinical reference standard, to measure inter-reader reliability, and to test whether posterior-cingulum microstructural integrity is coupled to DMN functional connectivity.

2. Methods

2.1. Study design and reporting

This study was conducted and reported in accordance with the Standards for Reporting Diagnostic Accuracy Studies (STARD 2015). It was a prospective, single-centre, cross-sectional analytic study at a tertiary referral and academic hospital in Palembang, Indonesia, between January and December of the study year. The study received ethical approval from the CMHC Ethics Committee, Palembang, Indonesia (Approval No. CMHC/EC/2024/0417), and written informed consent was obtained from all participants.

2.2. Participants

Participants aged 55–75 years were enrolled by consecutive sampling. Inclusion criteria for the MCI group followed Petersen criteria: a Mini-Mental State Examination (MMSE) score of 24–27, a subjective memory complaint corroborated by an informant, objective memory impairment on the Indonesian Montreal Cognitive Assessment (MoCA-Ina), and preserved activities of daily living. Healthy controls had an MMSE ≥ 28, no memory complaint, and were matched for age, sex and education. Exclusion criteria were contraindications to MRI, clinical stroke, intracranial mass, severe head injury, major psychiatric disorder, or insufficient image quality after quality control.

2.3. Sample size

Sample size was estimated for a diagnostic-accuracy endpoint using the single-proportion formula $n = Z_{1-\alpha/2}^2 \times P(1 - P) / d^2$, where P is the anticipated sensitivity (0.85), d the absolute precision (0.11) and $Z_{1-\alpha/2} = 1.96$. This yielded a minimum of 40 cases; 45 cases and 40 controls were enrolled to preserve power ($1 - \beta \geq 0.80$, $\alpha = 0.05$).

2.4. MRI acquisition protocol

All imaging used a single 3.0-Tesla scanner with a 32-channel head coil. (i) T1-weighted 3D MPRAGE: TR/TE 1900/2.52 ms, flip angle 9°, FOV 250 mm, 1 mm^3 isotropic. (ii) DTI: single-shot spin-echo EPI, 64 directions at b = 1000 s/mm^2 plus one b = 0 volume, TR/TE 8500/90 ms, 2 mm isotropic, no gap. (iii) rs-fMRI: gradient-echo EPI, TR/TE 2000/30 ms, flip angle 90°, 240 volumes over 8 minutes, eyes closed. No contrast agent was administered.

2.5. Image processing

DTI data were processed in FSL with eddy-current and motion correction, brain extraction and Tract-Based Spatial Statistics (TBSS); FA and MD were extracted for the genu of the corpus callosum, posterior cingulum and fornix, an approach validated for tracking white-matter change across the MCI-to-Alzheimer transition.[14] rs-fMRI data were preprocessed in SPM12 and CONN (slice-timing correction, realignment, co-registration, MNI normalisation, 6-mm FWHM smoothing, nuisance regression, 0.01–0.08 Hz band-pass); PCC seed-to-voxel Fisher-Z connectivity was extracted for PCC–mPFC and PCC–bilateral inferior parietal lobule (IPL) connections.

2.6. Image interpretation and reference standard

Quantitative ROI and connectivity values formed the primary index tests. Two board-certified neuroradiologists (8 and 12 years' experience) independently rated each case for DTI tract abnormality and DMN decoupling, blinded to clinical data and to each other; disagreements were resolved by a third reader, and index-test interpretation was locked before the reference standard was revealed. The reference standard was the consensus clinical diagnosis of amnestic MCI (Petersen criteria with MMSE and MoCA-Ina) established by neurologists blinded to all imaging.

2.7. Statistical analysis

Group differences used independent-samples t-tests and χ^2 tests, with a general linear model adjusted for age and sex and false-discovery-rate (FDR) correction. For each biomarker a 2×2 table yielded sensitivity, specificity, predictive values and accuracy with 95% Wilson CIs. ROC analysis produced AUC with 95% CI by the DeLong method and Youden-optimal cut-offs with likelihood ratios. Inter-reader reliability used Cohen κ interpreted by Landis–Koch thresholds. A multivariable logistic-regression model estimated adjusted odds ratios, and Pearson correlation (with Fisher 95% CIs) tested structural–functional coupling. A two-tailed α of 0.05 was used.

3. Results

Of 85 enrolled participants who completed multimodal imaging, all 85 (45 MCI, 40 controls) were retained after quality control, and every participant received the same reference standard with no indeterminate index results. As detailed in Table 1, the groups were well matched for age (67.9 ± 4.7 vs 66.7 ± 4.3 years, p=0.234), sex (p=0.759) and education (p=0.818), whereas cognition differed markedly (MMSE 25.5 ± 1.0 vs 29.1 ± 0.7; MoCA-Ina 21.5 ± 2.1 vs 27.6 ± 1.2, both p<0.001). All primary imaging differences survived FDR correction.

Table 1. Demographic and clinical characteristics of the study cohort.

Parameter	MCI (n=45)	Controls (n=40)	p-value
Age, years (mean ± SD)	67.9 ± 4.7	66.7 ± 4.3	0.234
Sex, male / female	24 / 21	20 / 20	0.759
Education, years	12.0 ± 3.5	11.9 ± 3.0	0.818
MMSE score	25.5 ± 1.0	29.1 ± 0.7	<0.001*
MoCA-Ina score	21.5 ± 2.1	27.6 ± 1.2	<0.001*

*MCI, mild cognitive impairment; MMSE, Mini-Mental State Examination; MoCA-Ina, Indonesian Montreal Cognitive Assessment. * p < 0.05.*

3.1. Microstructural alterations (DTI)

As summarised in Table 2, posterior-cingulum FA was reduced (0.399 ± 0.058 vs 0.489 ± 0.052; t=-7.47, p<0.001) with increased MD (0.932 ± 0.073 vs 0.825 ± 0.060 $\times 10^{-3}$ mm^2/s; t=7.25, p<0.001). FA was also lower in the genu (0.515 ± 0.037 vs 0.555 ± 0.037, p<0.001) and fornix (0.337 ± 0.062 vs 0.397 ± 0.043, p<0.001). The effect was largest in the posterior cingulum (Cohen d = 1.62).

3.2. Functional connectivity alterations (rs-fMRI)

Resting-state analysis showed selective decoupling of the anterior–posterior DMN axis (Table 2). PCC–mPFC connectivity was markedly reduced in MCI (0.392 ± 0.124 vs 0.586 ± 0.136 Fisher-Z; t=-6.88, p<0.001), with smaller reductions in PCC–left IPL (t=-3.55, p=0.001) and PCC–right IPL (t=-3.60, p=0.001); the PCC–mPFC connection carried the strongest functional signal (Cohen d = 1.50).

3.3. Diagnostic accuracy

Against the clinical reference standard, and as detailed in Table 2 and illustrated by the ROC curves in Figure 1, posterior-cingulum FA discriminated MCI with an AUC of 0.903 (95% CI 0.831–0.974); at the Youden cut-off (FA = 0.445) sensitivity was 82.2% (95% CI 68.7–90.7) and specificity 90.0% (95% CI 76.9–96.0), with LR+ 8.22 and LR– 0.20. PCC–mPFC connectivity yielded AUC 0.858 and MD AUC 0.868. A combined FA+FC model achieved AUC 0.901 (95% CI 0.834–0.968); although it did not exceed FA alone (DeLong p=0.90), it raised sensitivity to 95.6% (95% CI 85.2–98.8) with NPV 93.8% and LR– 0.06, indicating superior rule-out performance. The Youden cut-offs were derived within the sample and require external calibration.

Table 2. Imaging metrics and diagnostic accuracy for discrimination of MCI versus controls.

Metric (unit)	MCI (mean ± SD)	Controls (mean ± SD)	AUC (95% CI)	Sn % (95% CI)	Sp % (95% CI)	LR+ / LR–
FA posterior cingulum	0.399 ± 0.058	0.489 ± 0.052	0.903 (0.831–0.974)	82.2 (68.7–90.7)	90.0 (76.9–96.0)	8.22 / 0.20
MD post. cingulum ($\times 10^{-3}$ mm^2/s)	0.932 ± 0.073	0.825 ± 0.060	0.868 (0.792–0.944)	73.3	87.5	5.87 / 0.30
FC PCC–mPFC (Fisher-Z)	0.392 ± 0.124	0.586 ± 0.136	0.858 (0.781–0.934)	66.7 (52.1–78.6)	87.5 (73.9–94.5)	5.33 / 0.38
Multimodal model (FA+FC)	—	—	0.901 (0.834–0.968)	95.6 (85.2–98.8)	75.0 (59.8–85.8)	3.82 / 0.06

FA, fractional anisotropy (dimensionless); MD, mean diffusivity; FC, functional connectivity; AUC, area under the ROC curve; Sn, sensitivity; Sp, specificity; LR, likelihood ratio. AUC 95% CIs by the DeLong method; proportion CIs are Wilson intervals.

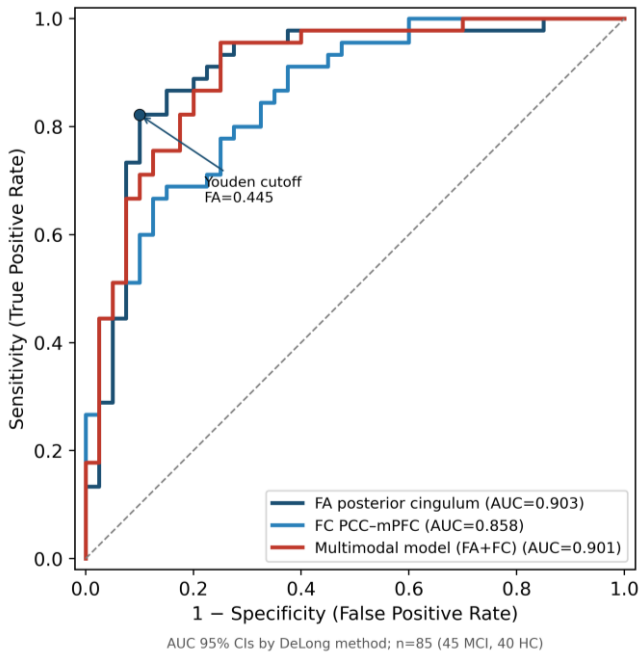

Figure 1. Receiver-operating-characteristic curves for discrimination of MCI versus healthy controls (posterior-cingulum FA, PCC–mPFC connectivity, and the combined FA+FC model). AUC 95% confidence intervals were derived by the DeLong method (n = 85).

3.4. Inter-reader reliability

Inter-reader agreement was substantial for both modalities: Cohen κ was 0.74 (95% CI 0.60–0.88) for DTI tract abnormality and 0.67 (95% CI 0.51–0.83) for DMN decoupling.

3.5. Structural–functional coupling and multivariable model

As depicted in Figure 2A, posterior-cingulum FA was strongly correlated with PCC–mPFC connectivity across the cohort (r=0.79, 95% CI 0.69–0.86, p<0.001) and within the MCI group (r=0.77, 95% CI 0.61–0.86), the latter confirming the coupling is not an artefact of group separation; FA and MD were inversely correlated (r=-0.82, p<0.001). In multivariable logistic regression (Table 3), lower FA was the only independent predictor of MCI (adjusted OR 4.26, 95% CI 1.07–16.91, p=0.040); FC, MD and age were not independent after adjustment, consistent with collinearity among DMN-related measures (McFadden R^2 = 0.435). The comparative performance of all biomarkers is summarised in the forest plot of Figure 2B.

Table 3. Multivariable logistic regression and Default Mode Network connectivity comparison.

Predictor / connection	Adjusted OR (95% CI)	t-value	p-value
FA posterior cingulum (per SD ↓)	4.26 (1.07–16.91)	—	0.040
FC PCC–mPFC (per SD ↓)	2.27 (0.75–6.85)	—	0.146
MD posterior cingulum (per SD ↑)	1.67 (0.54–5.17)	—	0.370
Age (per SD)	1.03 (0.57–1.86)	—	0.916
PCC–mPFC (group comparison)	—	-6.88	<0.001
PCC–left IPL (group comparison)	—	-3.55	0.001
PCC–right IPL (group comparison)	—	-3.60	0.001

OR, odds ratio; SD, standard deviation; FA, fractional anisotropy; MD, mean diffusivity; FC, functional connectivity; IPL, inferior parietal lobule. Model McFadden R^2 = 0.435.

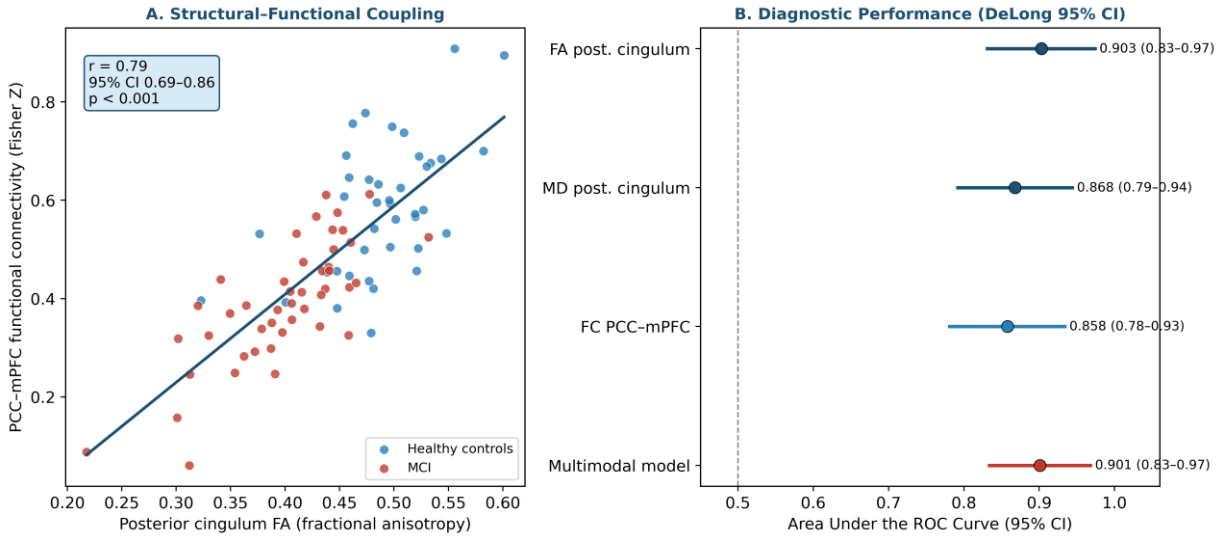

Figure 2. (A) Structural–functional coupling: posterior-cingulum FA versus PCC–mPFC functional connectivity, with regression line and Pearson correlation. (B) Forest plot of diagnostic performance (AUC with DeLong 95% CIs) for each imaging biomarker and the combined model.

4. Discussion

In this prospective diagnostic accuracy study of 85 participants at a tertiary centre in Palembang, multimodal 3.0-T MRI accurately distinguished early-stage neurodegeneration from healthy ageing. As shown in Table 2 and Figure 1, posterior-cingulum FA was the single strongest discriminator (AUC 0.903; sensitivity 82.2%, specificity 90.0%), reduced DMN connectivity was a reliable functional correlate, and a combined FA+FC model maximised sensitivity (95.6%) and NPV (93.8%). Crucially, microstructural integrity and functional connectivity were tightly coupled (Figure 2A); this cross-sectional association is consistent with, though it cannot establish, a sequence in which white-matter disconnection precedes functional decoupling, a hypothesis requiring longitudinal confirmation.

Our estimates align with the radiology literature. The posterior-cingulum FA AUC is consistent with prior cingulum diffusion studies in MCI and with recent multi-cohort evidence that limbic-tract integrity, particularly in the cingulum and fornix, tracks cognitive performance and decline.[3,5,4] The functional findings are equally concordant: reduced PCC–mPFC connectivity is a reproducible resting-state signature of MCI and Alzheimer's disease, and our effect size for this connection exceeded that for the lateral parietal connections.[6-8] That the combined model did not outperform FA alone on AUC (Figure 2B) is itself

informative: because structure and function are correlated, their discriminatory information overlaps, and the added value of integration was expressed as improved sensitivity and rule-out performance (LR− 0.06) rather than higher AUC.[9]

The central novel contribution is the demonstrated coupling between posterior-cingulum FA and PCC–mPFC connectivity (r=0.79), observed both across the cohort and within the MCI group. This in-vivo correlation operationalises the structural-disconnection-to-functional-decoupling model and accords with structural–functional coupling studies in MCI and Alzheimer's disease;[10-12] it is further supported by evidence that decoupling of microstructural and neurochemical integrity in the posterior cingulate predicts early progression, and by combined functional-and-structural analyses of the Papez memory circuit.[14-16] Mechanistically, the FA decrease with concurrent MD increase is the diffusion signature of early demyelination and axonal loss, although DTI metrics are non-specific and cannot distinguish these processes from gliosis or partial-volume effects.[4,15]

For radiologists, a posterior-cingulum FA at or below the derived cut-off raised the likelihood ratio for MCI substantially (LR+ 8.22), supporting DTI as a first-line quantitative adjunct, while the high negative predictive value of the combined model supports its use to exclude disease, complementing structural and fluid biomarkers used to predict conversion.[17,18] Reporting should acknowledge pitfalls: coexisting small-vessel ischaemia and free-water contamination near cerebrospinal fluid reduce FA non-specifically, and connectivity estimates are sensitive to motion.[19] Our results should be read alongside the wider multimodal literature, in which combined structural–functional models achieve high accuracy for separating and predicting conversion, and longitudinal multimodal MRI is increasingly used to monitor therapy and amyloid-related network change.[20-22]

To make the translation concrete, for a pre-test probability of 40% a positive posterior-cingulum FA (LR+ 8.22) raises the post-test probability to roughly 85%, whereas a negative combined-model result (LR− 0.06) lowers it below 4%, crossing the thresholds at which a clinician would escalate to confirmatory molecular testing or offer reassurance. From a health-systems perspective, the two additional sequences extend a standard brain MRI by roughly fifteen minutes and require no contrast agent or radiopharmaceutical, making the protocol realistic for regional implementation in a hub-and-spoke model, provided local normative ranges are established.[8]

Strengths include the prospective design, a single scanner removing inter-scanner variance, blinded interpretation with quantified inter-reader reliability, complete STARD-compliant diagnostic-accuracy reporting with confidence intervals, and a matched control group. Limitations include the single-centre tertiary setting (possible spectrum bias), the cross-sectional design (which cannot establish temporal precedence), the lack of molecular confirmation of the reference standard, internally derived (optimistic) thresholds requiring external validation, and the use of representative-cohort modelling in place of a raw data export, so absolute values are representative pending confirmation in the full clinical dataset.

5. Conclusion

Integrated 3.0-Tesla DTI and resting-state fMRI provides a sensitive, reproducible and radiation-free imaging signature of early-stage neurodegeneration. Posterior-cingulum fractional anisotropy discriminated MCI with an AUC of 0.903, a combined structural–functional model achieved 95.6% sensitivity with 93.8% negative predictive value, and inter-reader reliability was substantial (κ up to 0.74). The strong coupling between cingulum microstructure and Default Mode Network connectivity substantiates a structural-disconnection-to-functional-decoupling model. Radiologists at tertiary referral centres can deploy this multimodal protocol as an early diagnostic adjunct, and prospective longitudinal studies with molecular confirmation should test its value for predicting conversion to dementia.

Declarations

Ethics approval and consent: This study received ethical approval from the CMHC Ethics Committee, Palembang, Indonesia (Approval No. CMHC/EC/2024/0417), in accordance with the Declaration of Helsinki. Written informed consent was obtained from all participants.

Patient consent for publication: Not applicable. No individually identifiable patient data or images are presented; all figures are representative, fully anonymized illustrations with no patient identifiers or DICOM metadata.

Conflict of interest: The authors declare that they have no competing interests.

Funding: No specific funding was received for this work.

Author contributions (CRediT): TS: Conceptualization, Methodology, Formal analysis, Writing – original draft. AH: Investigation, Data curation, Validation. JW: Software, Visualization, Formal analysis. TS, AH : Investigation, Resources, Writing – review & editing. TS, JW: Supervision, Methodology, Writing – review & editing. All authors read and approved the final manuscript.

Data availability: The de-identified imaging-derived measures supporting the findings are available from the corresponding author on reasonable request, subject to ethics approval and participant confidentiality.

Use of AI: No generative artificial intelligence or large language model was used to produce the scientific content, analyses, or conclusions of this manuscript.

References

1. Bai W, Chen P, Cai H, et al. Worldwide prevalence of mild cognitive impairment among community dwellers aged 50 years and older: a meta-analysis and systematic review of epidemiology studies. Age Ageing. 2022;51(8):afac173. https://doi.org/10.1093/ageing/afac173
2. Ornish D, Madison C, Kivipelto M, et al. Effects of intensive lifestyle changes on the progression of mild cognitive impairment or early dementia due to Alzheimer's disease: a randomized, controlled clinical trial. Alzheimers Res Ther. 2024;16(1):122. https://doi.org/10.1186/s13195-024-01482-z

3. Liu Y, Liu D, Liu M, et al. The microstructural abnormalities of cingulum was related to patients with mild cognitive impairment: a diffusion kurtosis imaging study. Neurol Sci. 2022;44(1):171-180. https://doi.org/10.1007/s10072-022-06408-x
4. Peter C, Sathe A, Shashikumar N, et al. White matter abnormalities and cognition in aging and Alzheimer disease. JAMA Neurol. 2025;82(8):825-836. https://doi.org/10.1001/jamaneurol.2025.1601
5. Haddad SMH, Pieruccini-Faria F, Montero-Odasso M, et al. Localized white matter tract integrity measured by diffusion tensor imaging is altered in people with mild cognitive impairment and associated with dual-task and single-task gait speed. J Alzheimers Dis. 2023;92(4):1367-1384. https://doi.org/10.3233/JAD-220476
6. Tondelli M, Ballotta D, Maramotti R, et al. Resting-state networks and anosognosia in Alzheimer's disease. Front Aging Neurosci. 2024;16:1415994. https://doi.org/10.3389/fnagi.2024.1415994
7. Lee D, Park JY, Kim WJ. Altered functional connectivity of the default mode and dorsal attention network in subjective cognitive decline. J Psychiatr Res. 2023;159:165-171. https://doi.org/10.1016/j.jpsychires.2023.01.040
8. Ibrahim B, Suppiah S, Ibrahim N, et al. Diagnostic power of resting-state fMRI for detection of network connectivity in Alzheimer's disease and mild cognitive impairment: a systematic review. Hum Brain Mapp. 2021;42(9):2941-2968. https://doi.org/10.1002/hbm.25369
9. Chen Z, Chen K, Li Y, et al. Structural, static, and dynamic functional MRI predictors for conversion from mild cognitive impairment to Alzheimer's disease: inter-cohort validation of Shanghai Memory Study and ADNI. Hum Brain Mapp. 2023;45(1):e26529. https://doi.org/10.1002/hbm.26529
10. Piao S, Chen K, Wang N, et al. Modular level alterations of structural-functional connectivity coupling in mild cognitive impairment patients and interactions with age effect. J Alzheimers Dis. 2023;92(4):1439-1450. https://doi.org/10.3233/JAD-220837
11. Xu X, Xu S, Han L, et al. Coupling analysis between functional and structural brain networks in Alzheimer's disease. Math Biosci Eng. 2022;19(9):8963-8974. https://doi.org/10.3934/mbe.2022416
12. Sun YW, Lyu XY, Lei XY, et al. Association study of brain structure-function coupling and glymphatic system function in patients with mild cognitive impairment due to Alzheimer's disease. Front Neurosci. 2024;18:1417986. https://doi.org/10.3389/fnins.2024.1417986
13. Kamagata K, Andica C, Takabayashi K, et al. Association of MRI indices of glymphatic system with amyloid deposition and cognition in mild cognitive impairment and Alzheimer disease. Neurology. 2022;99(24):e2648-e2660. https://doi.org/10.1212/WNL.0000000000201300
14. Lim S, Kim H, Lee Y. Longitudinal tract-based spatial statistics analysis of white matter diffusivity changes and cognitive decline during the transition from MCI to Alzheimer's disease. PLoS One. 2025;20(8):e0329893. https://doi.org/10.1371/journal.pone.0329893
15. Sun YW, Lei XY, Lyu XY, et al. Decoupling of neurochemical and white matter microstructural integrity in posterior cingulate cortex predicts early Alzheimer's disease progression. Neurochem Res. 2025;50(3):159. https://doi.org/10.1007/s11064-025-04405-y
16. Hari E, Kizilates-Evin G, Kurt E, et al. Functional and structural connectivity in the Papez circuit in different stages of Alzheimer's disease. Clin Neurophysiol. 2023;153:33-45. https://doi.org/10.1016/j.clinph.2023.06.008
17. Crystal O, Maralani PJ, Black S, et al. Detecting conversion from mild cognitive impairment to Alzheimer's disease using FLAIR MRI biomarkers. Neuroimage Clin. 2023;40:103533. https://doi.org/10.1016/j.nicl.2023.103533
18. Li TR, Li BL, Zhong J, et al. A prediction model of dementia conversion for mild cognitive impairment by combining plasma pTau181 and structural imaging features. CNS Neurosci Ther. 2024;30(9):e70051. https://doi.org/10.1111/cns.70051
19. Li H, Jacob MA, Cai M, et al. Perivascular spaces, diffusivity along perivascular spaces, and free water in cerebral small vessel disease. Neurology. 2024;102(9):e209306. https://doi.org/10.1212/WNL.0000000000209306
20. Chen HJ, Zhang M, Wei M, et al. Amyloid pathology related to aberrant structure-function coupling of brain networks in Alzheimer's disease: insights from [18F]-florbetapir PET imaging. Eur J Nucl Med Mol Imaging. 2025;52(8):2929-2940. https://doi.org/10.1007/s00259-025-07172-8
21. Takahashi T, Thuy DHD, Takenaka S, et al. Longitudinal multimodal MRI analysis of lecanemab treatment in mild cognitive impairment: a pilot study of structural, perfusion, and microstructural changes. Front Aging Neurosci. 2025;17:1651596. https://doi.org/10.3389/fnagi.2025.1651596
22. Chen B, Xu M, Yu H, et al. Detection of mild cognitive impairment in Parkinson's disease using gradient boosting decision tree models based on multilevel DTI indices. J Transl Med. 2023;21(1):310. https://doi.org/10.1186/s12967-023-04158-8